Supporting Information

A porous Ti-based metal-organic framework for CO_2 photoreduction and imidazole-depended anhydrous proton conduction

Jian-Xin Qu,[a] Yao-Mei Fu,[b] Xing Meng,*[a] Yu-Ou He,[a] Hong-Xu Sun,[a] Rui-gang Yang,[a] Hai-Ning Wang,*[a] and Zhong-Min Su[b,c]

[a]School of Chemistry and Chemical Engineering, Shandong University of Technology, Zibo, 255049, China.

[b]Shandong Engineering Research Center of Green and High-value Marine Fine Chemical; Weifang University of Science and Technology, Shouguang, 262700, China.

[c]School of Chemistry and Environmental Engineering, Changchun University of Science and Technology, Changchun, 130022, China.

E-mail: mengxing837@foxmail.com; wanghn913@foxmail.com.

Experimental Section

Synthesis of IEF-11

The **IEF-11** was synthesized according to the literature. [S1]

Synthesis of Im@IEF-11

The obtained **IEF-11** was pretreated according to the ratio of 50 mL of dichloromethane per 500 mg of **IEF-11**, kept for three days and changed the solvent three times a day. Finally, the dichloromethane was poured out and the solid was dried under vacuum at 80°C for 8 hours. Next, different mass of imidazole and 100mg **IEF-11** were mixed homogeneously under N_2 atmosphere and kept in an oven at 100°C for 8h to obtain **Im@IEF-11-X** (X=100, 200 and 300, the representative mass of imidazole added was 100 mg, 200 mg and 300 mg, respectively). The obtained samples were cleaned by dichloromethane, and the final product was obtained after drying at 50 °C for a period of time.

Proton conduction test

The sample was placed in a homemade press die (10 mm in diameter), and the sample was pressed under a pressure of 0.6 MPa to obtain the block in the form of a round tablet. After measuring the thickness of the disc-shaped block, copper conductive adhesive is glued on both sides and fixed on the electrode. Alternating current (ac) impedance analyses are carried out on the compressed pellet samples to evaluate the proton conductivity.

Proton conductivity was calculated using the following equation:

$$\sigma = \frac{L}{R\,S}$$

Where L and S are the length (cm) and cross-sectional area (cm^2) of the samples respectively, and R, which was extracted directly from the impedance plots, is the bulk resistance of the sample (**Ω**). Activation energy (E_a) for the materials conductivity was estimated from the following equation:

$$ln(\sigma T) = lnA - \frac{Ea}{K_B T}$$

where σ is the electrical conductivity ($S \cdot cm^{-1}$) of the test material, A is the pre-exponential factor, K_B is the Boltzmann constant (eV/K), T is the test temperature (K), and E_a stands for the proton transport activation energy.

Photocatalytic reduction of CO_2 test

The photocatalytic reduction was tested in a home-made photocatalytic reactor. The LED lamp (40 W) was utilized as an irradiation source. The gas products were measured using gas chromatography (GC 1120) with an FID detector and a TCD detector.

Material characterization

The powder X-ray diffraction (PXRD) spectra were recorded on a Bruker D8 Advance X-ray diffractometer with Cu Kα radiation (λ = 1.5418 Å). Diffraction intensity data for 2θ from 5-70° were collected at the scanning speed of 10 deg/min. Fourier Transform Infrared Spectroscopy (FT-IR) spectroscopy was tested with FTIR-850 and KBr was used as the background. Scanning electron microscopy (SEM) images and scanning electron microscopy-energy dispersive spectrometer (SEM-EDS) analyses were carried out on Quanta 250 with an acceleration voltage of 10 kV. X-ray photoelectron spectroscopy (XPS) measurements were carried out on a scanning X-ray microprobe (K-Alpha, Thermo Scientific) with Al α radiation and the C 1s peak at 284.8 eV as the internal standard. Thermogravimetric was tested with STA 449 in the Nitrogen atmosphere. The UV-vis diffuse reflectance spectra (UV-vis DRS) were recorded on a Persee TU-1901 Spectrophotometer with $BaSO_4$ as reflectance standard from 200 to 800 nm. The Mott-Schottky and photoelectrochemical measurements were performed on a CHI 760E electrochemical workstation in 0.2 M Na_2SO_4 electrolyte with Ag/AgCl electrode as the reference electrode.

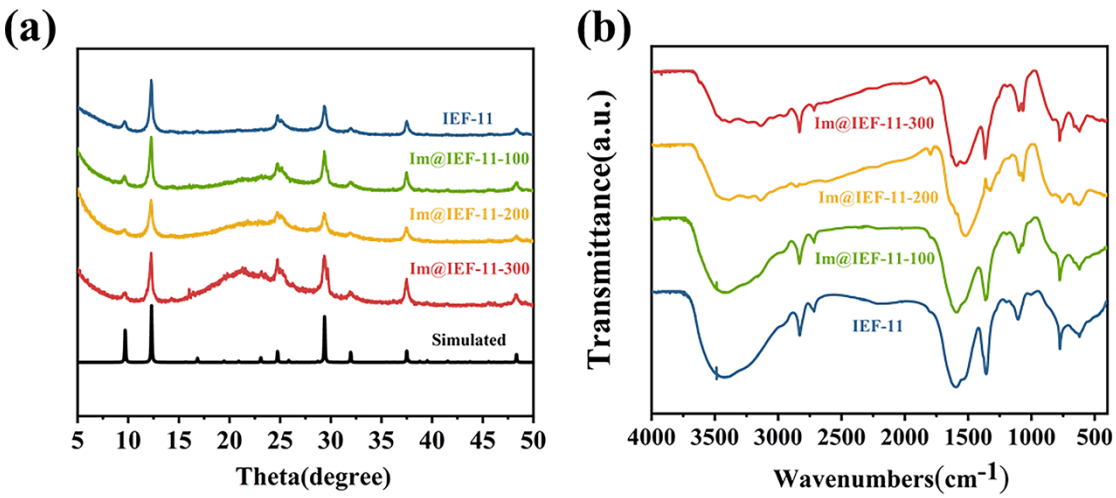

Fig. S1 (a) The PXRD patterns of simulated and as-synthesized **IEF-11** and **Im@IEF-11** and (b) the FT-IR spectra of **IEF-11** and **Im@IEF-11**.

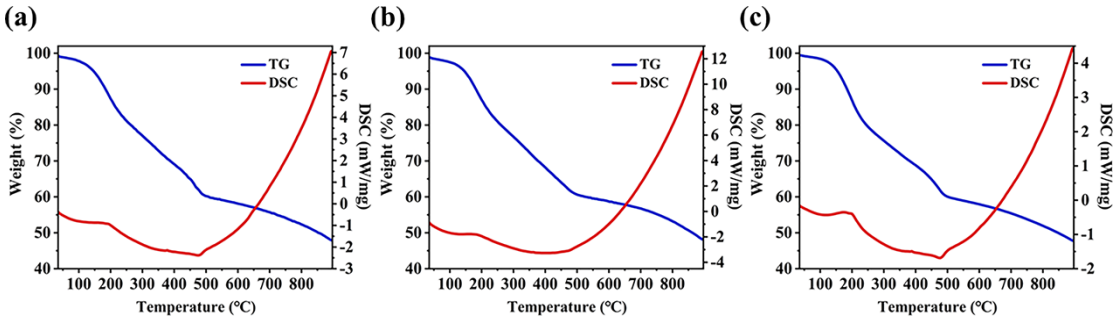

Fig. S2 The TG and DSC curve of **Im@IEF-11-100** (a), **Im@IEF-11-200** (b), and **Im@IEF-11-300** (c).

Im@IEF-11 were tested for thermogravimetric analysis (TG) and differential scanning calorimetry (DSC) (Fig. S2). The TG plots of **Im@IEF-11-X** reveal that the escape of imidazole molecules trapped in the channels of **IEF-11** starts at about 190 °C, then, after around 480 °C, the framework started to collapse. Considering that the melting point of the imidazole molecule is about 90 °C, this proves that the imidazole units are encapsulated in the pores of **IEF-11** rather than resting on the surface. The DSC test results show that there is an exothermic peak near 190 °C, belonging to the evaporation of imidazole molecules, and the heat absorption peak around 480 °C is attributed to the decomposition of the framework.

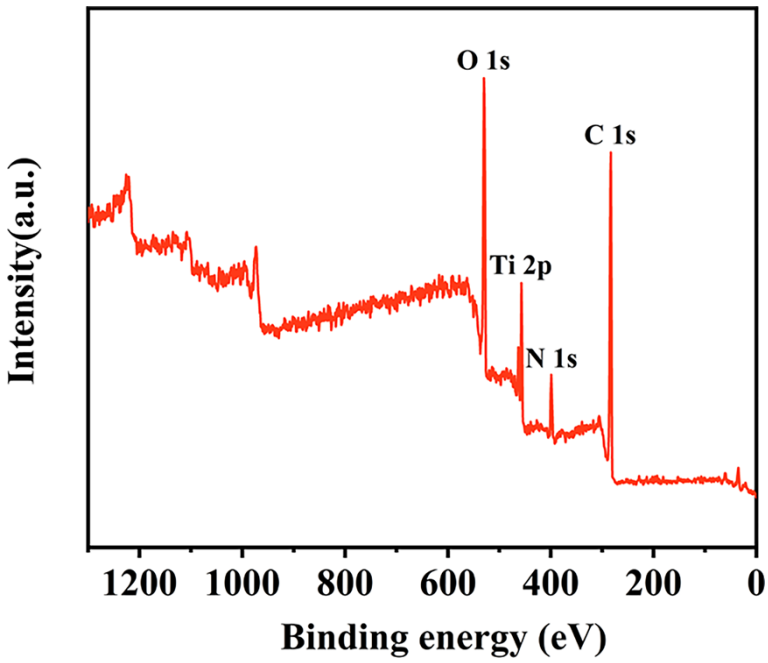

Fig. S3 The survey XPS spectra of **Im@IEF-11-200**.

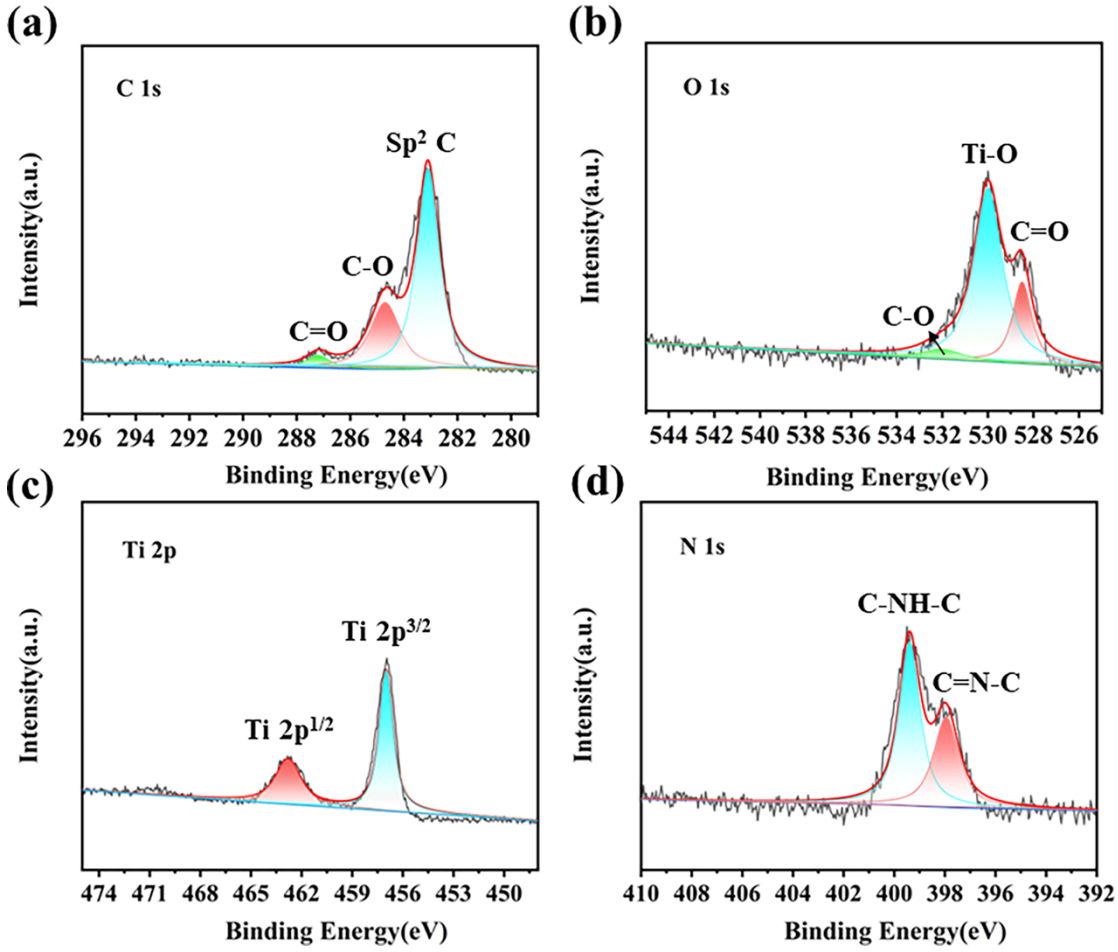

Fig. S4 High-resolution XPS spectra of for the C 1s (a), O 1s (b) Ti 2p (c) and N 1s (d) signals, recorded for the **Im@IEF-11-200** sample.

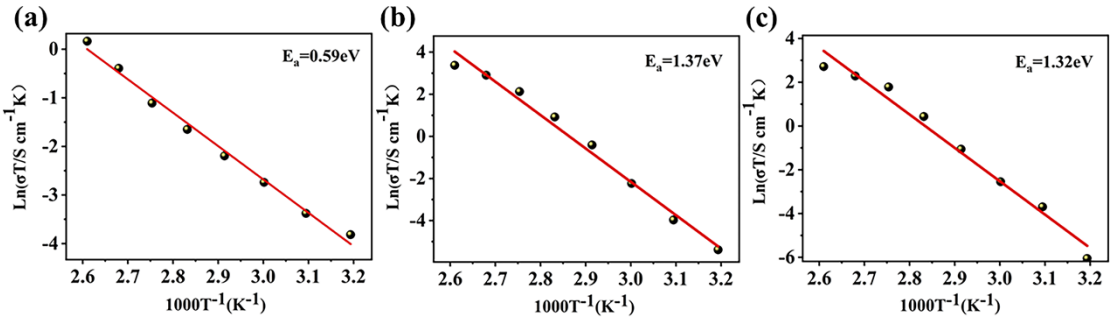

Fig. S5 Arrhenius plots of **Im@IEF-11-100** (a), **Im@IEF-11-200** (b) and **Im@IEF-11-300** (c).

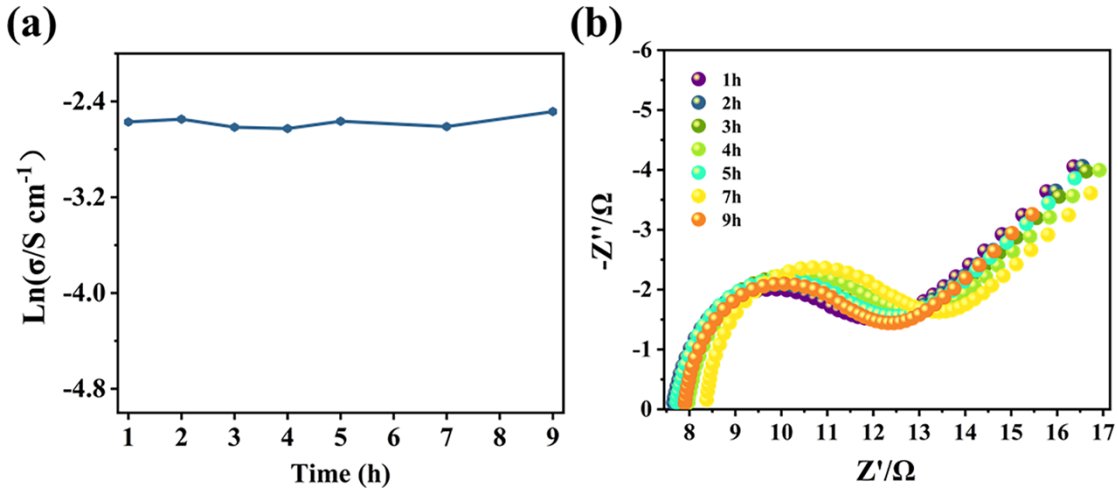

Fig. S6 (a) Proton conductivity and (b) Impedance spectra of **Im@IEF-11-200** at 110°C and anhydrous conditions.

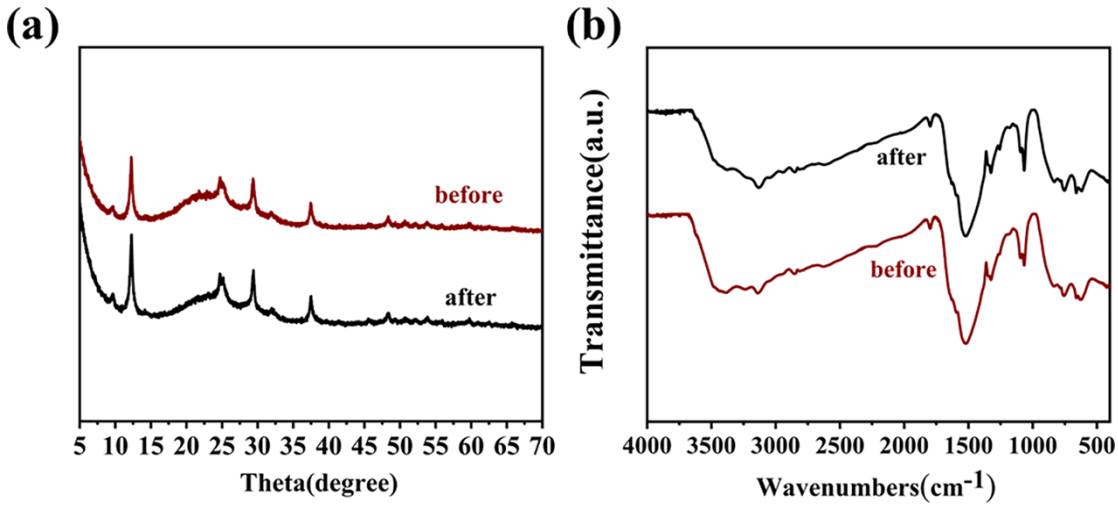

Fig. S7 (a) The PXRD patterns and (b) FT-IR spectra of **Im@IEF-11-200** before and after proton conductivity tests.

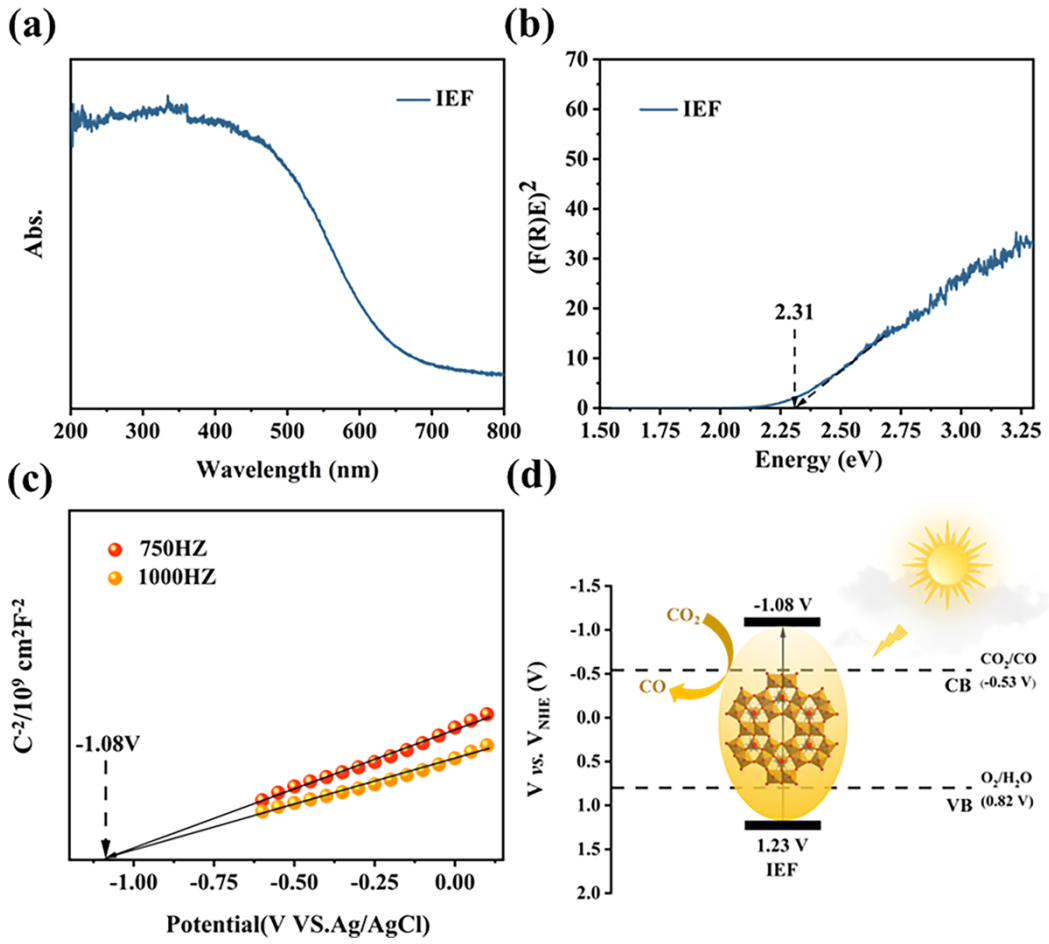

Fig. S8 (a) UV-vis diffuse-reflectance absorption spectra, (b) the band gap spectra, (c) Mott-Schottky plots and (d) the energy level diagram of **IEF-11**.

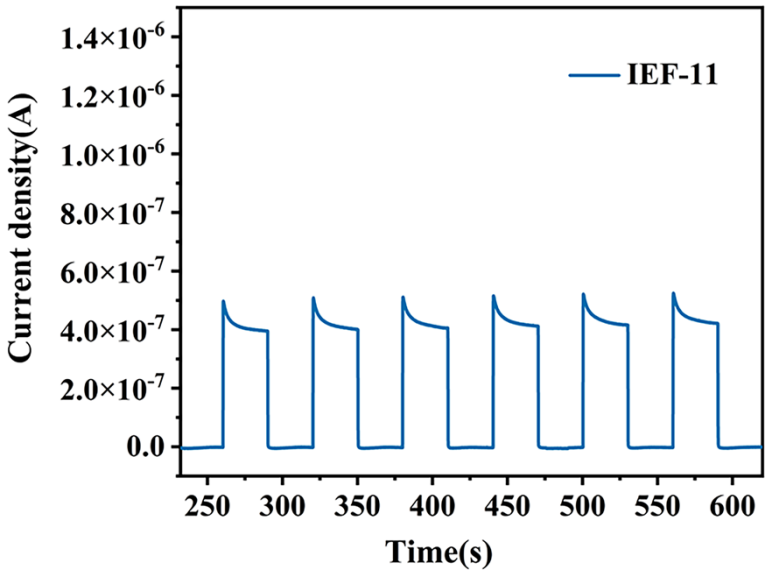

Fig. S9 Transient photocurrent response of **IEF-11**.

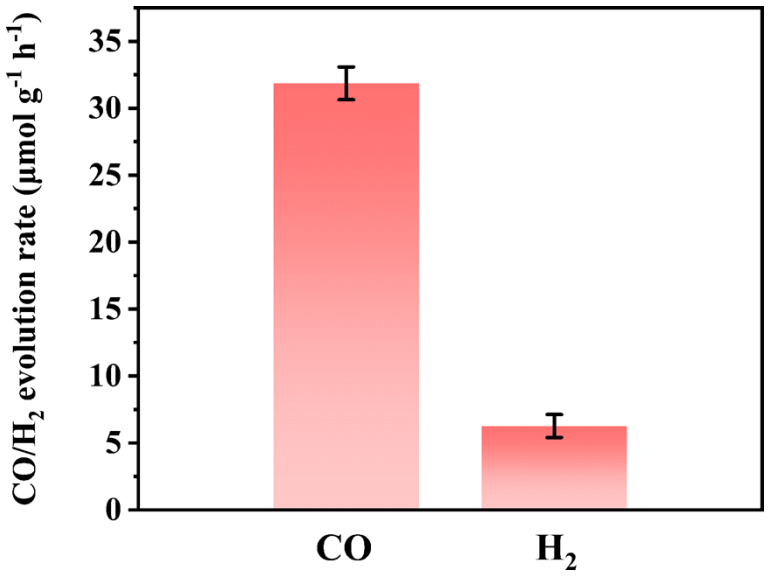

Fig. S10 CO and H_2 formation rates of **IEF-11**. (The repeated experiments are conducted for three times.)

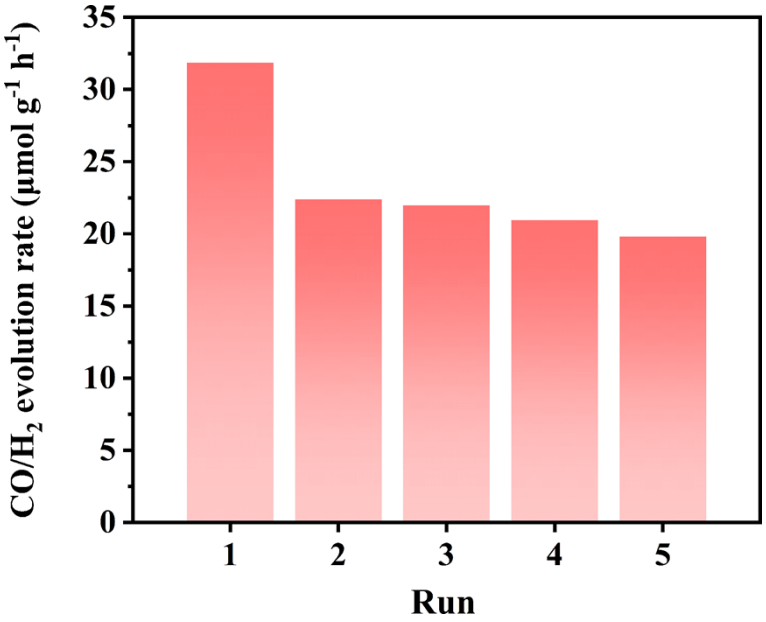

Fig. S11 The 4-cycle test of **IEF-11**.

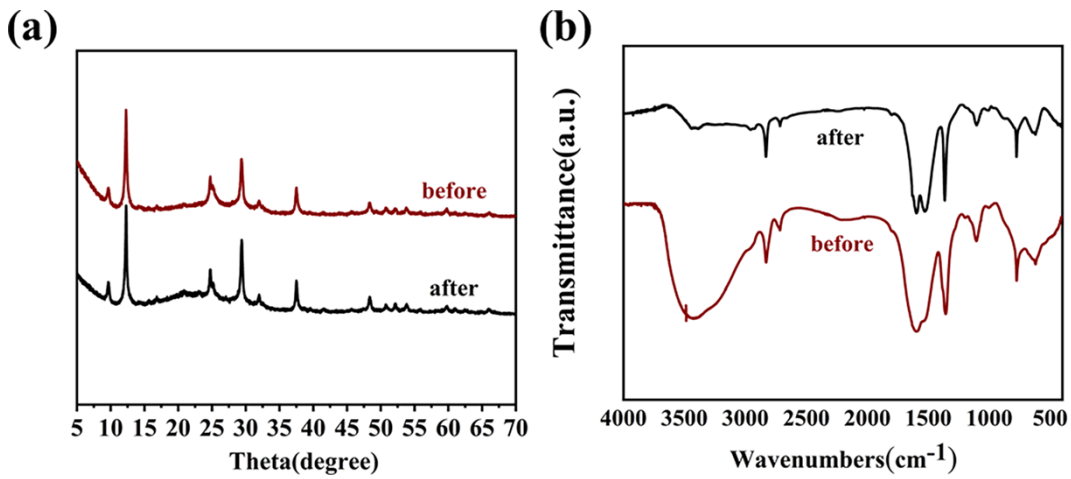

Fig. S12 (a) The PXRD patterns and (b) FT-IR spectra of **Im@IEF-11-200** before and after photocatalytic test.

Table S1 Proton conductivity of MOF-based composites under anhydrous conditions.

Materials	Proton conductivity (S cm^{-1})	Condition	Ref.
GO@UiO-66-NH_2/Nafion	3.403×10^{-3} S·cm^{-1}	120˚C	S2
$[Cu_{12}(12L_4H_3SO_4)\ (I)_{12}(3pz{\cdot}2H_3SO_4)]_n$	3.80×10^{-3} S·cm^{-1}	80˚C	S3
$\{[Gd_2(CO_3)\ (ox)_2(H_2O)_2]{\cdot}3H_2O\}_n$	1.98×10^{-3} S·cm^{-1}	150˚C	S4
SA-EIMS@MIL-101	1.89×10^{-3} S·cm^{-1}	150˚C	S5
$(NH_4)_3[Zr(H_{2/3}PO_4)_3]$	1.45×10^{-3} S·cm^{-1}	180˚C	S6
(Me_2NH_2) [Eu (PHIA)]	1.30×10^{-3} S·cm^{-1}	150˚C	S7
(Me_2NH_2) [Eu(L)]	1.25×10^{-3} S·cm^{-1}	150˚C	S7
$[Zn(HPO_4)\ (H_2PO_4)_2]\ (ImH_2)_2$-TfH-10	3.00×10^{-4} S·cm^{-1}	110˚C	S8
Im@CuBTC	1.04×10^{-4} S·cm^{-1}	70˚C	S9

Table S2 Ti based MOFs photocatalysts for CO_2 photocatalytic reduction.

Photocatalyst	Product	Catalytic activity	Ref.
MIP-208@RuO_x	CH_4	33.33 μmol g^{-1} h^{-1}	S10
RuO_x@MIL-125(Ti)–NH_2	CH_4	840.91 μmol g^{-1} h^{-1}	S11
Bi_2S_3@NH_2-MIL-125(Ti)-SH	CO	12.46 μmol g^{-1} h^{-1}	S12
NH_2-MIL-125(Ti) MOF/g-C_3N_4	CO	95.95 μmol g^{-1} h^{-1}	S13
	CH_4	3.48μmol g^{-1} h^{-1}	
RGO-NH_2-MIL-125(Ti)	CH_3OH	1966.67 μmol g^{-1} h^{-1}	S14
NH_2-MIL-125-Ni	CO	5.1 μmol g^{-1} h^{-1}	S15
Ag NP-loaded NH_2-MIL-125(Ti)	CO	26.7 μmol g^{-1} h^{-1}	S16
	CH_4	63.3 μmol g^{-1} h^{-1}	
TiO_2/NH_2-MIL-125(Ti)	CH_4	1.18 μmol g^{-1} h^{-1}	S17
D-TiMOF	CO	59.55 μmol g^{-1} h^{-1}	S18

Reference

[S1] P. Salcedo-Abraira, A. A. Babaryk, E. Montero-Lanzuela, O. R. Contreras-Almengor, M. Cabrero-Antonino, E. S. Grape, T. Willhammar, S. Navalon, E. Elkaim, H. Garcia and P. Horcajada, *Adv. Mater.*, 2021, **33**, 2106627.

[S2] Z. Rao, K. Feng, B. B. Tang and P. Y. Wu, *J. Membr. Sci.*, 2017, **533**, 160-170.

[S3] S. Khatua, A. Kumar Bar, J. Ahmad Sheikh, A. Clearfield and S. Konar, *Chem. Eur. J.*, 2018, **24**, 872-880.

[S4] Q. Tang, Y. L. Yang, N. Zhang, Z. Liu, S. H. Zhang, F. S. Tang, J. Y. Hu, Y. Z. Zheng and F. P. Liang, *Inorg. Chem.*, 2018, **57**, 9020-9027.

[S5]: H. Chen, S. Y. Han, R. H. Liu, T. F. Chen, K. L. Bi, J. B. Liang, Y. H. Deng and C. Q. Wan, *J. Power Sources*, 2018, **376**, 168-176.

[S6] D. X. Gui, X. Dai, Z. T. Tao, T. Zheng, X. X. Wang, M. A. Silver, J. Shu, L. H. Chen, Y. L. Wang, T. T. Zhang, J. Xie, L. Zou, Y. H. Xia, J. J. Zhang, J. Zhang, L. Zhao, J. Diwu, R. H. Zhou, Z. F. Chai and S. A. Wang, *J. Am. Chem. Soc.*, 2018, **140**, 6146-6155.

[S7]Y. S. Wei, X. P. Hu, Z. Han, X. Y. Dong, S. Q. Zang and T. C. W. Mak, *J. Am. Chem. Soc.*, 2017, **139**, 3505-3512.

[S8] S. Horike, D. Umeyama, M. Inukai, T. Itakura and S. Kitagawa, *J. Am. Chem. Soc.*, 2012, **134**, 7612-7615.

[S9] G. A. Bodkhe, M. A. Deshmukh, H. K. Patil, S. M. Shirsat, V. Srihari, K. K. Pandey, G. Panchal, D. M. Phase, A. Mulchandani and M. D. Shirsat, *J. Phys. D: Appl. Phys.*, 2019, **52**, 335105.

[S10] S. J. Wang, M. Cabrero-Antonino, S. Navalón, C. C. Cao, A. Tissot, I. Dovgaliuk, J. Marrot, C. Martineau-Corcos, L. Yu, H. Wang, W. Shepard, H. García and C. Serre, *Chem*, 2020, **6**, 3409-3427.

[S11] M. Cabrero-Antonino, B. Ferrer, H. G. Baldoví and Sergio Navalón, *Chem. Eng. J.*, 2022, **455**, 136426.

[S12] H. Wang, Q. Zhang, J. J. Li, J. Y. Zhang, Y. F. Liu, M. Zhou, N. Zhang, Y. Z. Fang and Q. F. Ke, *J. Colloid Interface Sci.*, 2022, **606**, 1745-1757.

[S13] R. R. Ikreedeegh and M. Tahir, *J. Environ. Chem. Eng.*, 2021, **9**, 105600.

[S14] J. O. Olowoyo, U. Saini, M. Kumar, H. Valdés, H. Singh, M. O. Omorogie, J. O. Babalola, A. V. Vorontsov, U. Kumar and P. G. Smirniotis, *J. CO2 Util.*, 2022, **42**, 101300.

[S15] S. Y. Chen, G. T. Hai, H. Y. Gao, X. Chen, A. Li, X. W. Zhang and W. J. Dong, *Chem. Eng. J.*, 2021, **406**, 126886.

[S16] X. M. Cheng, P. Wang, S. Q. Wang, J. Zhao and W. Y. Sun, *ACS Appl. Mater. Interfaces*, 2022, **14**, 32350-32359.

[S17] J. M. Hu, J. Ding and Q. Zhong, *J. Colloid Interface Sci.*, 2020, **560**, 857-865.

[S18] S. Y. Chen, F. C. Yang, H. Y. Gao, J. Y. Wang, X. Chen, X. W. Zhang, J. Li and A. Li, *J. CO2 Util.*, 2021, **48**, 101528.